Advanced Computational Tools for the Characterization of the Dynamic Response of MHD Control Systems in Large Fusion Devices

Paolo Bettini[1,2], Tommaso Bolzonella[2], Maurizio Furno Palumbo[1,2], Stefano Mastrostefano[3], Go Matsunaga[4], Ruben Specogna[5], Manabu Takechi[4], and Fabio Villone[3]

[1]Dipartimento di Ingegneria Industriale, Università di Padova, Padua 35131, Italy
[2]Consorzio RFX, Padua 35127, Italy
[3]Associazione EURATOM/ENEA/CREATE, Dipartimento di Ingegneria Elettrica e dell'Informazione, Università di Cassino e del Lazio Meridionale, Cassino 03043, Italy
[4]Japan Atomic Energy Agency, Naka 311-0193, Japan
[5]Dipartimento di Ingegneria Elettrica, Gestionale e Meccanica, Università di Udine, Udine 33100, Italy

The development of methods for the active control of magnetohydrodynamic (MHD) instabilities and the correction of error fields is mandatory in view of robust magnetic confinement in future fusion reactors. Two numerical codes (CAFE, CARIDDI) have been used to simulate the dynamic response of MHD control systems in large fusion devices. Their main pros and cons are discussed. As reference test case, the frequency domain characterization of a key system for MHD control in the large JT-60SA fusion device, namely the resistive wall mode active coil set, is considered.

Index Terms— **Eddy currents, fusion devices, magnetohydrodynamic (MHD), resistive wall mode (RWM).**

I. Introduction

THE dynamics of fusion plasmas is often conveniently described by magnetohydrodynamic (MHD) equations, which predict that some deviations from equilibrium may evolve as violent instabilities [1]. Among them, the appearance of resistive wall mode (RWM) instabilities critically depends on the characteristics of the conductive structures surrounding the plasma and in particular on their non-uniformities [2].

The growth rate typical of RWMs enables the use of sophisticated feedback control strategies by means of active coils. Experimentally, in the presence of closed-loop control actions, eddy currents in 3-D conducting structures and plasma perturbations will evolve in a coupled way. In addition, the controller design itself needs an accurate evaluation of all the dynamical effects due to the non-uniformities of the passive boundary during the control coil action [3].

A quantitative comprehension of all these interaction represents, therefore, a challenging problem for the numerical modeling related to any fusion device design and operation [4]–[6].

This paper is focused on the characterization of the dynamic response of the resistive wall mode coil (RWMC) system of the JT-60SA experiment [7], [8], an innovative large tokamak device being built as joint international project between Japan and Europe. One of the most important missions of JT-60SA is to pursue fully non-inductive steady-state operations with high values of the plasma pressure exceeding the so-called no-wall ideal MHD stability limits. To reach this ambitious target, effective MHD control system tools have to be implemented in the device, including RWM control system. RWM feedback control in JT-60SA relies on 18 saddle coils installed on the plasma side of the stabilizing plate (SP), a double-wall structure made of two stainless steel shells (10 mm thick, 70 mm air gap). In previous works, simplified (2-D) electromagnetic analyses have been performed to help the identification of the requirements for the power supply system [9]. Here, a full 3-D characterization of the dynamic response of the RWMC system, crucial for quantitatively assessing the control effectiveness of the real experiment, will be presented.

Manuscript received May 23, 2014; revised September 3, 2014; accepted September 15, 2014. Date of current version April 22, 2015. Corresponding author: P. Bettini (e-mail: paolo.bettini@unipd.it).

Color versions of one or more of the figures in this paper are available online at http://ieeexplore.ieee.org.

Digital Object Identifier 10.1109/TMAG.2014.2360158

II. Computational Tools

Two numerical codes (CAFE [10], CARIDDI [11]) have been used to characterize the dynamic response of the MHD control system in JT-60SA, in presence of complex 3-D conducting structures surrounding the plasma.

These codes are based on alternative edge element formulations (discrete and integral, respectively) for 3-D eddy current computation. Details and pros and cons of the proposed formulations are reported in the following.

A. CAFE

In the code CAFE, a discrete geometric formulation is implemented, based on line integral of the magnetic vector potential over generic polyhedra. In the numerical domain D, three sub-domains are identified: 1) D_c, which includes all the conductive passive structures surrounding the plasma (further details in Section III); 2) D_a, which includes the non-conductive regions (vacuum and air); and 3) D_s, which includes all the active coils used to control the plasma instabilities. The domain D is covered by a hexahedral mesh, whose incidences are encoded in the cell complex K represented by the standard incidence matrices $\boldsymbol{G}$, $\boldsymbol{C}$, and $\boldsymbol{D}$ [12]. A dual barycentric complex $\tilde{K}$ is obtained from K using the

barycentric sub-division; its incidence matrices are $\tilde{\boldsymbol{G}} = \boldsymbol{D}^T$, $\tilde{\boldsymbol{C}} = \boldsymbol{C}^T$, and $\tilde{\boldsymbol{D}} = -\boldsymbol{G}^T$. When modeling stranded coils, and this is the case, it is advisable to introduce integral sources to provide a good accuracy without covering D_s with a fine mesh.

Then, the circulations of the magnetic vector potential $\boldsymbol{A}$ along primal edges $e \in D$ can be expressed as $\boldsymbol{A} = \boldsymbol{A}_r + \boldsymbol{A}_s$, where $\boldsymbol{A}_r$ is the circulation of the magnetic vector potential due to eddy currents in D_c (reaction field) and $\boldsymbol{A}_s$ is the circulations of the magnetic vector potential produced by the sources in D_s.

By combining the discrete Ampère's and Faraday's laws with the discrete counterpart of the constitutive laws for the flux density $\boldsymbol{B}$ and current density $\boldsymbol{J}$, a symmetric complex linear system of equations is obtained [10]

$$(\boldsymbol{C}^T \boldsymbol{\nu} \boldsymbol{C} + i\omega\boldsymbol{\sigma})\boldsymbol{A}_r = -i\omega\boldsymbol{\sigma}\boldsymbol{A}_s \tag{1}$$

where ω is the angular frequency, and $\boldsymbol{\nu}$ and $\boldsymbol{\sigma}$ are square matrices based on mesh element geometry, material properties, and hypothesis on the fields to be computed. Each entry of $\boldsymbol{A}_s$ in the RHS of (1) is computed with standard closed formulas in D_c and zero otherwise.

The main advantage of this formulation is that the symmetric linear system (1) is very sparse (non-zero entries are $\sim$5%). Therefore, it can be solved efficiently with a standard *tree-cotree gauge* up to some millions of unknowns [some hundred thousands degrees of freedom (DoFs) ascribed to the conductive regions], using a state-of-the-art direct solver.[1]

According to the precision required, the results (reaction fields) can be computed directly by interpolation inside each mesh element or by a post-processing procedure, via Biot–Savart law (parallel implementation in OpenMP).

The main disadvantage of this formulation is related to the mesh generation itself (Section III).

B. CARIDDI

The code CARIDDI [11] is based on an integral formulation of the eddy currents problem in non-magnetic conductors V_c. Assuming a time-harmonic dependence with angular frequency ω, the electric field $\mathbf{E}$ is given by

$$\mathbf{E} = -j\omega\mathbf{A} - \nabla\varphi \tag{2}$$

where the magnetic vector potential $\mathbf{A}$ (such that $\mathbf{B} = \nabla \times \mathbf{A}$) is computed from the current density $\mathbf{J}$ via Biot–Savart law. We then give a weak form of Ohm's law

$$\int_{V_c} \eta\mathbf{J} \cdot \mathbf{w}\, dV + j\omega \int_{V_c} \mathbf{A} \cdot \mathbf{w}\, dV + \int_{V_c} \nabla\phi \cdot \mathbf{w}\, dV = 0 \tag{3}$$

where $\mathbf{w}$ is a suitable test function belonging to the same functional space as $\mathbf{J}$ and η is the resistivity (a tensor for anisotropic conductors). To assure that the current density is solenoidal, the electric vector potential $\mathbf{T}$ is introduced such that $\mathbf{J} = \nabla \times \mathbf{T}$, with a two-component gauge [11].

From the numerical point of view, we give a finite element discretization of V_c and we use edge elements $\mathbf{N}_k$ to expand $\mathbf{T}$, to guarantee the correct continuity conditions in presence of non-homogeneous conductors

$$\mathbf{T} = \sum_k I_k \mathbf{N}_k \Rightarrow \mathbf{J} = \sum_k I_k \nabla \times \mathbf{N}_k. \tag{4}$$

The gauge condition is imposed with a tree-cotree decomposition of the mesh [11]. Complex topologies of V_c and equipotential electrodes are treated as described in [13]. Solving (3) with the Galerkin method, we have

$$(j\omega \underline{\underline{L}} + \underline{\underline{R}})\underline{I} = \underline{\underline{D}}\,\underline{V} \tag{5}$$

$$L_{i,j} = \frac{\mu_0}{4\pi} \int_{V_c}\int_{V_c} \frac{\nabla \times \mathbf{N}_i(\mathbf{r}) \cdot \nabla \times \mathbf{N}_j(\mathbf{r}')}{|\mathbf{r} - \mathbf{r}'|} dV dV' \tag{6}$$

$$R_{i,j} = \int_{V_c} \nabla \times \mathbf{N}_i \cdot \eta \cdot \nabla \times \mathbf{N}_j dV \tag{7}$$

$$D_{i,j} = -\int_{\Sigma_j} \nabla \times \mathbf{N}_i \cdot \hat{\mathbf{n}}\, dS \tag{8}$$

where $\underline{I}$ is the vector of DoFs I_k defined in (4), and $\underline{V}$ is the vector of voltages applied to electrodes Σ_j having $\hat{\mathbf{n}}$ as normal unit vector.

The main advantage of this method is that only a mesh of the conducting domain is needed, which is very convenient in fusion devices, where plasma, air, and vacuum volumes far exceed those of the conducting structures. In addition, the formulation is ready to be coupled to a plasma response matrix [14] to get a full state-space linearized representation of the overall system made of the plasma and surrounding conducting structures. On the other hand, the matrices to be inverted to solve the problem (5) are fully populated. This limits the maximum number of mesh elements (usually up to some tens of thousands) and requires resorting to fast and parallel techniques for addressing large scale problems [15].

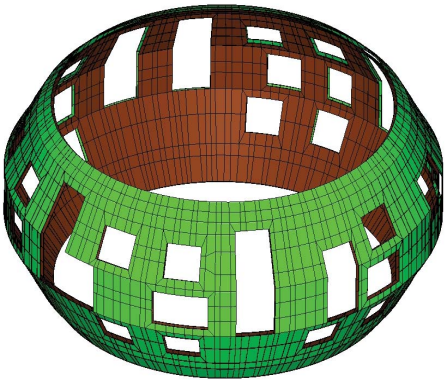

Fig. 1. Actual geometry with full account of non-axisymmetric conducting structures (here only the SP is shown).

III. Numerical Results

A. 3-D Geometry and Mesh

The computational domain has been obtained, starting from a CAD description of the JT60-SA device,[2] by adopting

[1] PARDISO, Intel MKL library.

[2] Modeled by means of CATIA v5 software.

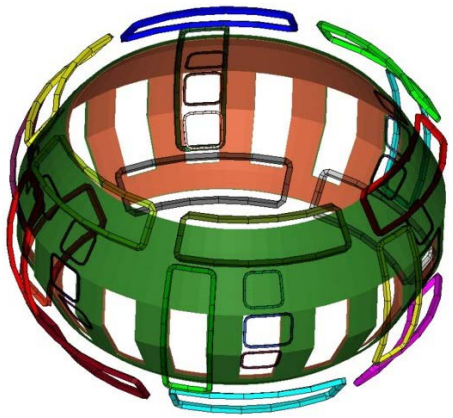

Fig. 2. Reference geometry with symmetric conducting structures. The SP is shown, together with actual control coils (RWMC, EFCC).

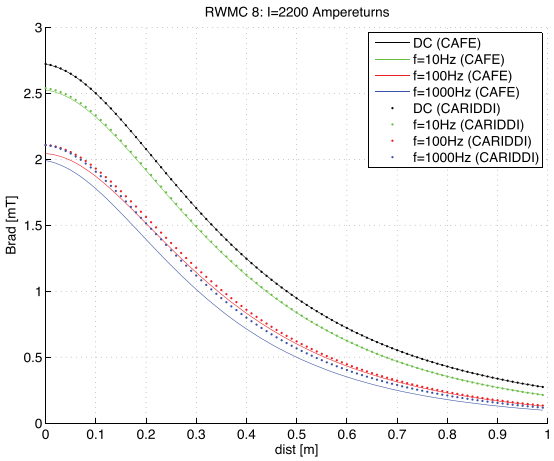

Fig. 3. Amplitude of the magnetic flux density as a function of the distance from the center of RWMC nr. 8 (radial direction).

a sophisticated 3-D mesh generation strategy[3] to produce several meshes, with different assumptions on symmetry and increasing levels of accuracy for mesh sensitivity analysis.

The structures considered in the present analysis are the following.

1) *The SP (Fig. 1):* the main component for the passive stabilization of the plasma instabilities, composed by two shells with stiffening ribs,[4] all made of stainless steel SS316L. The SP presents many holes for vacuum systems, diagnostics, and external heating systems.
2) *The VV:* the hermetically sealed stainless steel container, which surrounds the plasma and houses the fusion reactions; it includes inspection ports and stiffening ribs. Presently, vacuum vessel (VV) is modeled without holes.
3) *The RWMCs:* installed on the inner side of the SP, consist of 18 coils made of oxygen free copper C1020, placed before some ports, which provide an active stabilization effect against the plasma instabilities (frequency range up to 3 kHz).
4) *The Error Field Correction Coils (EFCC):* placed between SP and VV, complement the active control system.[5]

The main difficulty of 3-D modeling of the machine (both CAD and mesh generation) is represented by the lack of symmetry of the conducting structures (in particular as far the SP is concerned, Fig. 1).

To exploit the main benefits of both approaches, cross-checks and validations are carried out on a simplified reference geometry, as described in Section III-B, whereas the analysis with full non-axisymmetric conducting structures are carried out with CARIDDI in Section III-C, avoiding the effort of meshing also plasma, air, and vacuum regions.

[3]A fully hexahedral mesh is obtained by means of a block partitioning of the computational domain using Hypermesh v12 software.

[4]In the present analysis, the SP is modeled without stiffening ribs in CARIDDI; it has been adopted an isotropic equivalent resistivity to take into account the volume occupied by these components.

[5]Note that the reference design of the equatorial array of EFCC has recently been slightly modified, but this not affects the results presented this paper that refers to the RWMC system.

B. Cross-Checks and Validations

A reference geometry, with symmetric conducting structures [20° symmetry cell (Fig. 2)], is introduced to allow a reliable cross-check of the results between the two numerical codes and an easier evaluation of the effects of including/neglecting some parts of the machine.

As required by any FEM-like code, in the model for CAFE analysis, the non-conductive region has also been discretized. In particular, it has been identified an air volume surrounding the structures of the device (36 m tall, 20 m wide) to apply the regularity conditions at infinity.

The high number of solids resulting from CAD model has been discretized by hexahedral elements to get a fully structured mesh that meets all the requirements in terms of Jacobian, aspect ratio, and absence of any self-intersections. The numerical domain has been discretized in 1 157 712 hexahedra[6] for the code CAFE: despite the relatively high number of unknowns (∼2.5 millions), the solution of (1) takes <800 s on a workstation equipped with two 8-core Xeon processors (2.7 GHz). The integral formulation uses a hexahedral mesh made of 24 576 elements. Since the number of unknowns is rather small (25 528), a serial version of CARIDDI has been used to compute the magnetic field. The computation of matrices (6)–(8) takes ∼1000 s on an Intel I7 processor (3.2 GHz). The results of the two codes are presented in Fig. 3 in terms of magnetic field along a given path (a radial line starting from the center of a coil—RWMC nr. 8—toward the center of the machine). The comparison shows a fairly good agreement, hence increasing confidence about the reliability of the geometrical model and of the results in frequency domain. In addition, this approach allows evaluating the influence of the different level of details adopted to model the conducting structures (e.g., SP with and w/o ribs): a discrepancy is visible at the highest frequencies, but it remains rather small (far below 10%). A detail of the eddy currents induced in SP and VV elements is shown in Fig. 4 (results of CAFE calculations at 100 Hz).

[6]1 048 524 elements for air/vacuum, 99 828 for the VV and 9360 for the SP.

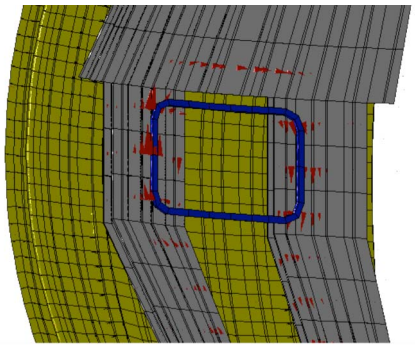

Fig. 4. Eddy current pattern (red cones) along SP (gray areas) and VV (yellow areas) elements. Active coil: RWMC nr. 8 (blue areas), 100 Hz.

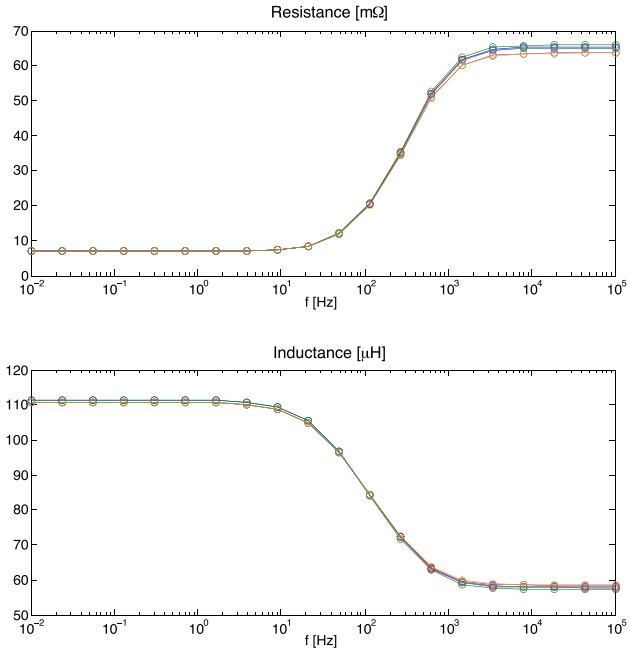

Fig. 5. Resistance (top) and inductance (bottom) of active RWM coils (upper set) as a function of the frequency.

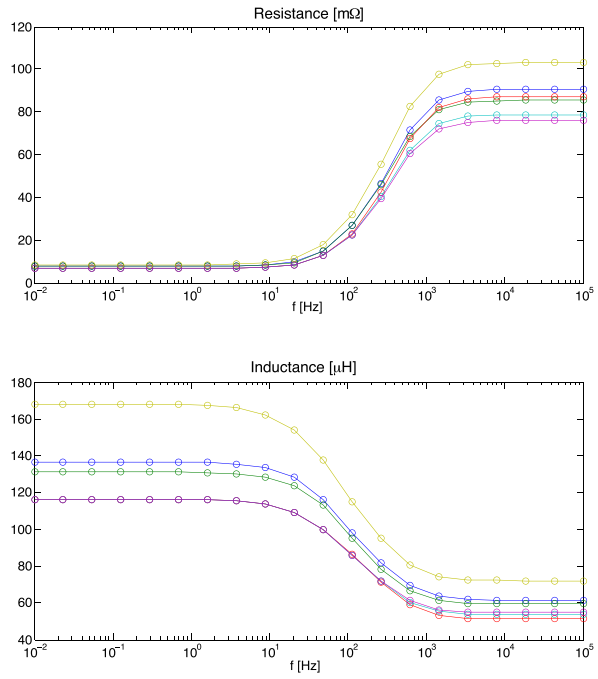

Fig. 6. Resistance (top) and inductance (bottom) of active RWM coils (equatorial set) as a function of the frequency.

C. Results

The actual model of the machine is considered, considering the non-axisymmetries of the conducting structures (in particular, SPs holes and ports). The integral formulation is adopted to evaluate the impedances of RWM coils, as a function of frequency, with straightforward computations.

Indeed, indicating with suffix p all the DoF of passive conductors (vessel and SP) and with suffix a the active conductors (RWM control coils), we obtain

$$\begin{aligned}\left(j\omega \underline{\underline{L}}_{pp} + \underline{\underline{R}}_{pp}\right)\underline{I}_p + j\omega \underline{\underline{L}}_{pa}\underline{I}_a = 0\\ j\omega \underline{\underline{L}}_{ap}\underline{I}_p + \left(j\omega \underline{\underline{L}}_{aa} + \underline{\underline{R}}_{aa}\right)\underline{I}_a = \underline{\underline{D}}\,\underline{V}_a.\end{aligned} \quad (9)$$

Simple algebraic manipulations on (9) and the observation that matrix $\underline{\underline{D}}$ is made of 0's and ± 1's, lead to

$$\begin{aligned}&\underline{\underline{Z}}_{aa}\underline{I}_a = \underline{V}_a\\ &\underline{\underline{Z}}_{aa} = j\omega\left[\underline{\underline{L}}_{aa} - j\omega \underline{\underline{L}}_{ap}\left(j\omega \underline{\underline{L}}_{pp} + \underline{\underline{R}}_{pp}\right)^{-1}\underline{\underline{L}}_{pa}\right] + \underline{\underline{R}}_{aa}\end{aligned} \quad (10)$$

so that $\underline{\underline{Z}}_{aa}$ can be interpreted as the impedance matrix of the active conductors. Figs. 5 and 6 report the behavior of the diagonal term of such matrix as a function of frequency, being the inductance L and resistance R defined as

$$L = \mathrm{Im}\left(\mathrm{diag}\left(\left(\frac{\underline{\underline{Z}}_{aa}}{2\pi f}\right)\right)\right) \quad R = \mathrm{Re}\left(\mathrm{diag}\left(\underline{\underline{Z}}_{aa}\right)\right). \quad (11)$$

Each plot reports six traces, corresponding to the six different coils along the toroidal angle for the set of upper and equatorial RWM coils. The upper RWM coils (Fig. 5) show a rather symmetric behavior. Conversely, some more noticeable differences arise on the equatorial RWM coils (Fig. 6). The differences at low frequencies are due to different geometrical dimensions of these coils, while at higher frequencies, further differences are ascribed to different current density patterns induced in the SP, due to non-symmetric positioning of holes and ports along the toroidal angle [360° model (Fig. 1)].

IV. Conclusion

In this paper, we have presented a comparison between two numerical codes (CAFE, CARIDDI) used to characterize the dynamic response of the MHD control systems in a large fusion device (JT-60SA). The preliminary results are in fairly good agreement. The model has proved to be as mature as required for next steps toward full plasma response models.

Acknowledgment

This work was supported by the Italian Ministry of Education and Research through the Projects of National Interest under Grant 2010SPS9B3.

REFERENCES

[1] G. Bateman, *MHD Instabilities*. Cambridge, MA, USA: MIT Press, 1978.

[2] M. S. Chu and M. Okabayashi, "Stabilization of the external kink and the resistive wall mode," *Plasma Phys. Control. Fusion*, vol. 52, no. 12, p. 123001, 2010.

[3] G. Marchiori, M. Baruzzo, T. Bolzonella, Y. Q. Liu, A. Soppelsa, and F. Villone, "Dynamic simulator of RWM control for fusion devices: Modelling and experimental validation on RFX-mod," *Nucl. Fusion*, vol. 52, no. 2, p. 023020, 2012.

[4] F. Villone, Y. Q. Liu, R. Paccagnella, T. Bolzonella, and G. Rubinacci, "Effects of three-dimensional electromagnetic structures on resistive-wall-mode stability of reversed field pinches," *Phys. Rev. Lett.*, vol. 100, p. 255005, Jun. 2008.

[5] M. Baruzzo *et al.*, "3D effects on RWM physics in RFX-mod," *Nucl. Fusion*, vol. 51, no. 8, p. 083037, 2011.

[6] T. Bolzonella, V. Igochine, S. C. Guo, D. Yadikin, M. Baruzzo, and H. Zohm, "Resistive-wall-mode active rotation in the RFX-mod device," *Phys. Rev. Lett.*, vol. 101, p. 165003, Oct. 2008.

[7] S. Ishida, P. Barabaschi, Y. Kamada, and the JT-60SA Team, "Overview of the JT-60SA project," *Nucl. Fusion*, vol. 51, no. 9, p. 094018, 2011.

[8] Y. Kamada *et al.*, "Plasma regimes and research goals of JT-60SA towards ITER and DEMO," *Nucl. Fusion*, vol. 51, no. 7, p. 073011, 2011.

[9] A. Ferro, E. Gaio, M. Takechi, M. Matsukawa, and L. Novello, "Studies on the requirements of the power supply system for the resistive-wall-mode control in JT-60SA," *Fusion Eng. Design*, vol. 88, nos. 9–10, pp. 1509–1512, 2013.

[10] P. Bettini, L. Marrelli, and R. Specogna, "Calculation of 3-D magnetic fields produced by MHD active control systems in fusion devices," *IEEE Trans. Magn.*, vol. 50, no. 2, Feb. 2014, Art. ID 7000904.

[11] R. Albanese and G. Rubinacci, "Integral formulation for 3D eddy-current computation using edge elements," *IEE Proc. A*, vol. 135, no. 5, pp. 457–462, Sep. 1988.

[12] E. Tonti, *The Mathematical Structure of Classical and Relativistic Physics*. Basel, Switzerland: Birkhäuser, 2013.

[13] G. Rubinacci, A. Tamburrino, and F. Villone, "Circuits/fields coupling and multiply connected domains in integral formulations," *IEEE Trans. Magn.*, vol. 38, no. 2, pp. 582–584, Mar. 2002.

[14] A. Portone, F. Villone, Y. Liu, R. Albanese, and G. Rubinacci, "Linearly perturbed MHD equilibria and 3D eddy current coupling via the control surface method," *Plasma Phys. Control. Fusion*, vol. 50, no. 8, p. 085004, 2008.

[15] G. Rubinacci, S. Ventre, F. Villone, and Y. Liu, "A fast technique applied to the analysis of resistive wall modes with 3D conducting structures," *J. Comput. Phys.*, vol. 228, no. 5, pp. 1562–1572, 2009.